

Freely Jointed Polymers Made of Droplets

Angus McMullen,¹ Miranda Holmes-Cerfon,² Francesco Sciortino,³ Alexander Y. Grosberg,¹ and Jasna Brujic¹

¹*Physics Department, New York University, New York, New York 10003, USA*

²*Courant Institute of Mathematical Sciences, New York University, New York, New York 10003, USA*

³*Dipartimento di Fisica, Sapienza Università di Roma, Rome, Italy*



(Received 10 May 2018; published 26 September 2018)

An important goal of self-assembly is to achieve a preprogrammed structure with high fidelity. Here, we control the valence of DNA-functionalized emulsions to make linear and branched model polymers, or “colloidomers.” The distribution of cluster sizes is consistent with a polymerization process in which the droplets achieve their prescribed valence. Conformational statistics reveal that the chains are freely jointed, so that the Kuhn length is close to one bead diameter. The end-to-end length scales with the number of bonds N as N^ν , where $\nu \approx 3/4$, in agreement with the Flory theory in two dimensions. The chain diffusion coefficient D approximately scales as $D \propto N^{-\nu}$, as predicted by the Zimm model. Unlike molecular polymers, colloidomers can be repeatedly assembled and disassembled under temperature cycling, allowing for reconfigurable, responsive matter.

DOI: [10.1103/PhysRevLett.121.138002](https://doi.org/10.1103/PhysRevLett.121.138002)

Experimental models of molecular polymers on the colloidal [1–7] or granular length scales [8–14] have been proposed in the literature. These studies have demonstrated how particle specificity, shape anisotropy, or nonequilibrium interactions can lead to the formation of chains. Assembly occurs either through thermal agitation, or the particles are aligned by external drives, such as gravity, capillarity, shaking, or magnetic and electric fields [10,15]. Despite these innovative proofs-of-concept, it remains an experimental challenge to design particles that self-assemble into flexible chains in bulk, leading to analogues of polymer solutions on different length scales.

Here we demonstrate a promising avenue for self-assembly, in which thermal activation leads to the polymerization of DNA-coated droplet monomers into chains, i.e., “colloidomerization.” The process of chain growth follows random aggregation, such that the average weight of the colloidomers and its statistical distribution can be predicted theoretically. These colloidal polymers allow for the visualization of micron-sized monomers, a length scale that is inaccessible in molecular systems. Having access to the conformational dynamics of a large pool of chains allows us to study their statistical physics.

While polymer theories have been validated at the single-molecule level using DNA imaging and force spectroscopy [16–18], our experimental model system examines whether these theories hold on colloidal length scales. The most important advantage of using droplets instead of solid particles as the monomer units is that the DNA bonds between them are fully mobile along the droplet surface. The droplets can therefore rearrange after binding and dynamically explore their equilibrium structures on a time-scale fixed by the droplet diffusion constant. Therefore, these

colloidomers behave like freely jointed polymers. By contrast, solid colloidal polymers can have limited flexibility [5,15,19]. Flexible DNA-linked colloids have been synthesized in several different ways [1,2,20–23]. Here, we utilize that flexibility to make flexible colloidal polymers in bulk.

We find excellent agreement between the data and the scaling exponents predicted by the Flory theory of 2D freely jointed chains with excluded volume, down to a chain size of only a handful of droplets. The self-diffusion coefficient of the colloidomers follows the Zimm scaling with length, highlighting the importance of hydrodynamic interactions.

One important difference between colloidomers and molecular polymers is that their particulate nature allows us to control monomer interactions to trigger chain assembly, disassembly, and reconfiguration. For example, here we show that cycling temperature to melt and reassemble the DNA bonds between the droplets can produce statistically similar distributions of chains. Previously, we have shown that the linear sequence of droplets with different DNA flavors can be programmed via DNA toe-hold displacement reactions [2]. In the future, these chains will serve as backbones for colloidal folding into complex 3D structures via secondary interactions, as proposed in Refs. [9,24].

To achieve a good yield and high fidelity of chains, we synthesize thermal droplets with a uniform coverage of sticky DNA, ensuring both fast dynamics and valence control. We make monodisperse PDMS droplets using a method adapted from Ref. [25] and outlined in detail in Ref. [2] (see Ref. [21] for a similar process). After we synthesize the droplets, we incubate them with a variable amount of binding DNA. As shown in Fig. 1(a), the DNA

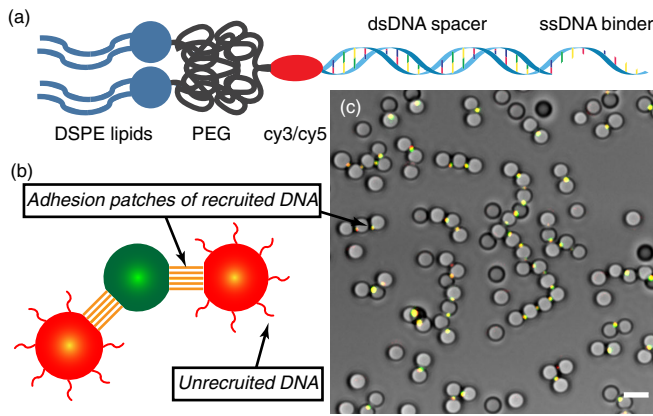


FIG. 1. (a) A schematic of the DNA-lipid construct grafted on the droplet. (b) Mixing emulsions with complementary DNA strands leads to their binding to form a trimer. (c) A bright-field image overlaid with a fluorescence image shows adhesions in self-assembled droplet chains. Scale bar is $5 \mu\text{m}$.

binders are comprised of a pseudorandom spacer of 50 bases, followed by a binding sequence of 20 bases, with one complementary strand labeled with a Cy3 and the other with a Cy5 fluorophore (see Ref. [26]—which includes Refs. [27,28]—for DNA sequences, designed with software from Ref. [29]). This molecule is then reacted with a lipid (DSPE-PEG2000-DBCO, Avanti) via the copper-free ring-strain promoted alkyne-azide cycloaddition reaction [30,31]. The hydrophobic part of the lipid anchors the DNA strands to the surface of the droplet. We react an additional strand, complementary to the random spacer prior to the sticky end, with another lipid molecule. This DNA-lipid complex hybridizes with that of the spacer of the binding DNA strand, anchoring the entire complex via two lipid molecules instead of one [32]. This prevents the migration of DNA from droplet to droplet; the fluorescence intensity remains stable throughout the experiment. The droplet buoyancy pins them close to the glass surface of the sample cell, confining the dynamics to two dimensions.

A droplet functionalized with single-stranded DNA binds to a complementary strand on another droplet [1,33–35] through DNA hybridization of the single-stranded (sticky) ends, as shown in Fig. 1(b). The choice of two distinctly functionalized droplets to make a heterocopolymer (instead of a homopolymer) plays also a crucial role in decreasing, if not suppressing, aggregates with minimal closed loops. The adhesion patch has a much higher density of DNA than on the perimeter of the droplet, as shown by the colocalized fluorescent signal in the vicinity of droplet contacts in Fig. 1(c). Since the density of DNA that can be recruited into a single patch is limited by geometry, any remaining DNA on the surface of the droplet can form a second patch with another droplet. Starting with a 1:1 mixture of complementary droplets at an area fraction ≈ 0.2 , we observe that the reaction rate of droplet-droplet binding increases linearly with the bulk DNA concentration up to $C_{\text{DNA}} = 2 \text{ pmol}$,

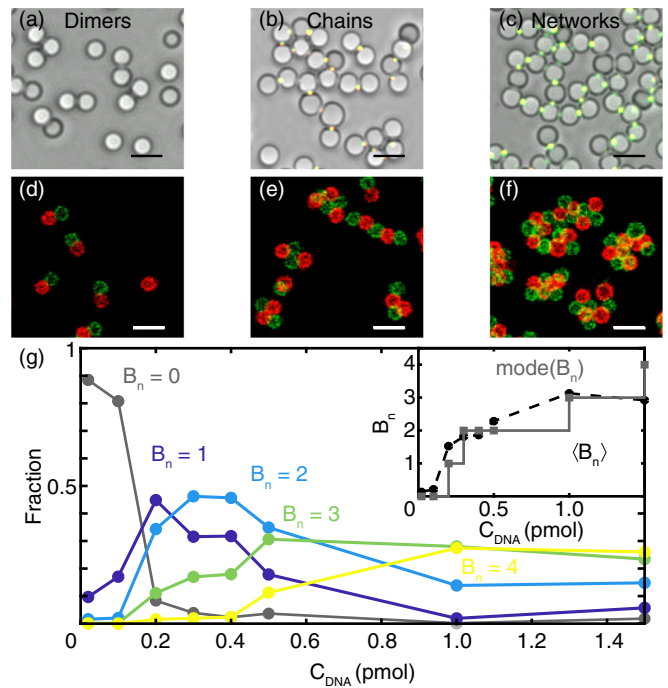


FIG. 2. Bright-field [(a),(b),(c)] and fluorescence [(d),(e),(f)], images of droplet structures show an increase in valence as a function of C_{DNA} . Attaching DNA via fluorescent streptavidin [26] in panels (d),(e),(f) instead of the chemistry described in the main text does not change our results. Scale bars are $5 \mu\text{m}$. (g) The number of bonds per droplet B_n increases with C_{DNA} , as shown by the average and the mode of the distributions in the inset.

above which the rate plateaus [26], as expected. Therefore, the assembly process reaches a steady state after a week for low C_{DNA} down to a day for high C_{DNA} .

Empirically, at steady state we observe an increase in droplet valence as a function of C_{DNA} , from dimers in Figs. 2(a),2(d), through chains in 2(b),2(e), to cross-linked networks in 2(c),2(f), resembling fibrous gels [36]. For a given C_{DNA} , we track the droplets in 2D over time [37] to determine the evolution of the droplet bond network. We consider two droplets bound only if their bond persists over 1 min, consistent with the fact that DNA bonds are practically irreversible at room temperature.

Figure 2(g) shows the fraction of droplets with a given bond number B_n at steady state, as a function of C_{DNA} . The spread in B_n at a given C_{DNA} may arise from nonuniform DNA coverage between droplets, any residual polydispersity, or kinetic or steric bottlenecks that prevent the droplets from reaching their prescribed valence. The inset in Fig. 2(d) shows that the average B_n increases smoothly with concentration, while the mode (the most probable B_n value) exhibits a stepwise increase, allowing us to tune the self-assembly.

Optimizing for valence two at $C_{\text{DNA}} = 0.2 \text{ pmol}$, the droplets assemble into linear or branched polymers in 63% of structures, while 28% of droplets remain unreacted monomers, and 9% constitute aggregates with higher valencies. The distribution of cluster sizes is shown by

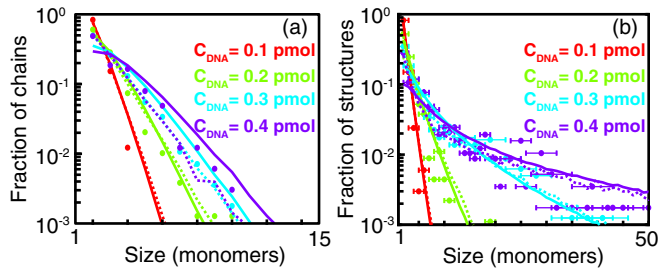


FIG. 3. Distribution of structure sizes for linear chains (a) and all clusters (b) for the indicated given loadings. The solid lines are predictions of the RBM, while dashed lines are the results of a Monte Carlo simulation. The horizontal error bars in (b) indicate monomer bin size.

the distributions in Fig. 3(a) for the subset of clusters that are in linear chains and in Fig. 3(b) for all structures. We compare these observed distributions to both a random branching model and to Monte Carlo simulations, assuming in both cases the experimentally measured valence distribution as an input. The random branching model [26,38] computes the size distribution of colloidomers assuming that they do not form loops, that monomers attach independently, and that each colloidomer is saturated, with no unused bonds [26]. Monte Carlo simulations mimic the experiment following the procedure outlined in Ref. [26].

The close agreement between the experimental results, the random branching model (RBM), and the Monte Carlo simulations, implies that the self-assembly is a random process, which goes to completion with minimal steric or kinetic inhibition. Using the measured valence distribution as the only input, the models reproduce the experimental distributions of linear chains and cluster sizes in steady state, as shown in Fig. 3. The data and simulations are fully consistent with an exponential distribution of linear chain lengths, while the RBM underestimates the fraction of short chains due to a lack of dynamics in the model. In all cases, the characteristic chain length increases with bulk C_{DNA} , offering the possibility to generate long chains and test the scaling relations of flexible colloidal polymers.

This result lends support to the hypothesis that each droplet has a valence prescribed by the concentration of DNA molecules on its surface. Fluctuations in the amount of DNA on each droplet likely arise from the inhomogeneous loading of the DNA from the bulk onto the droplets, resulting in an initial distribution of valence.

In contrast to molecular polymers, colloidomers can be disassembled upon heating above the DNA melting temperature and reassembled into statistically similar chains upon cooling, as shown by the reversible valence distribution in Fig. 4. The exponential decay in the fraction of monomers (black line) in response to the cooling temperature ramp reveals a rate of droplet binding of $1/7$ min, such that the B_N distribution reaches a steady state after only 20 min. The fast reassembly is due to the presence of pluronic surfactant (F68) in the system. At high temperatures, the

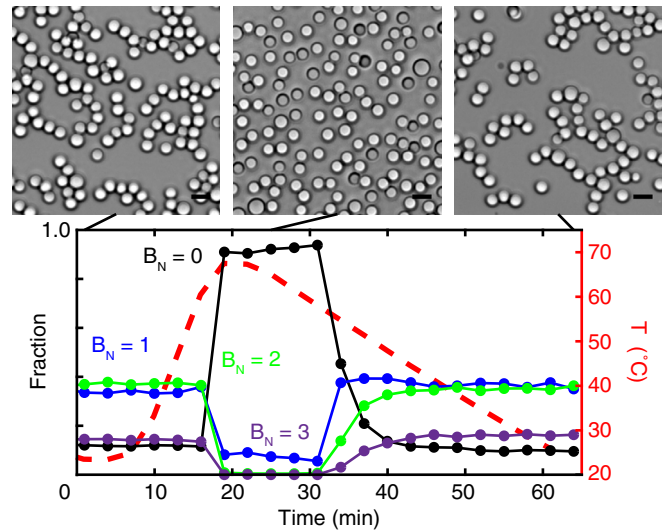


FIG. 4. Evolution of the bond number distribution of a sample as a function of time under the temperature ramp shown in red. The corresponding images of the droplet structures are shown above. Scale bar is $5 \mu\text{m}$.

surfactant causes a weak depletion between droplets, increasing the assembly rate far beyond that observed at room temperature [26]. This evidence of reversibility in the droplet valence is in agreement with the numerical prediction that aggregation (aging) dynamics is similar to that occurring in equilibrium for systems with a low valence [39,40]. The possibility to manipulate droplet-droplet bonds by temperature or using specific DNA reactions [41] presents a useful tool to configure colloidomer solutions *in situ*.

Next, we investigate the conformational statistics of trimers in two dimensions to test whether the droplet-droplet bonds are freely jointed. The bond angle subtended by the centers of the two end-cap droplets on the center of the middle droplet is shown in the inset in Fig. 5(b). Apart from the angle ($\pi/3$) excluded on both sides of the center droplet, the histogram in the Fig. 5(a) shows that droplets explore bond angles with a flat probability. To characterize the

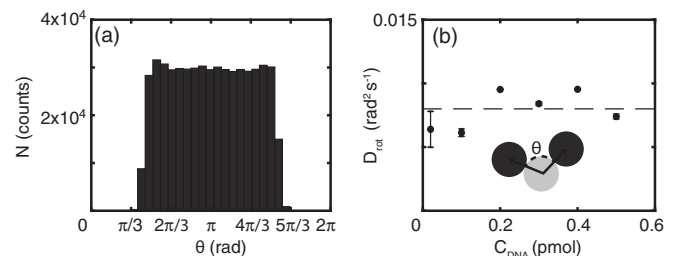


FIG. 5. (a) A histogram of the explored angular configurations of 876 trimers, corrected for out of plane motion. Angles above ($\pi/3$) and below ($5\pi/3$) are allowed. (b) The measured angular diffusion coefficient for the bond reorganization as a function of the DNA loading density. There is no correlation between DNA loading density and bond viscosity.

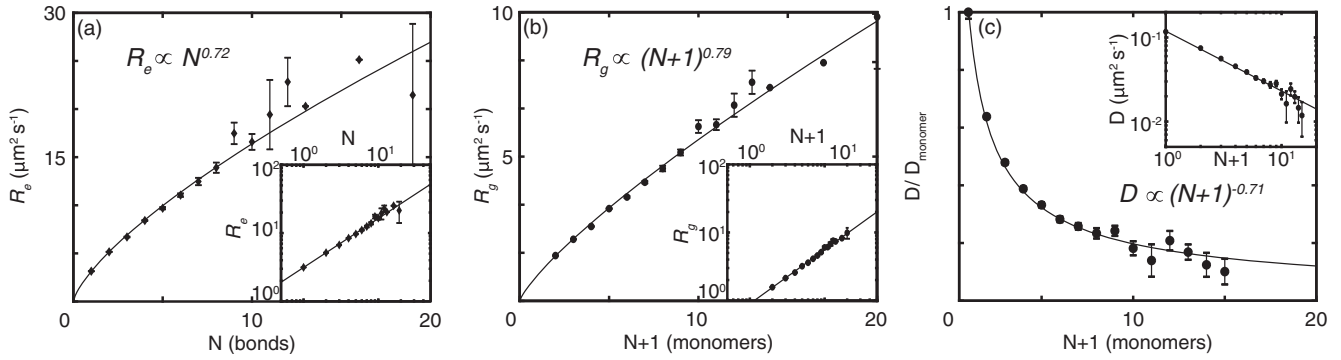


FIG. 6. Plots of the (a) R_e , (b) R_g , and (c) D , normalized by the diffusion of a single monomer ($0.12 \mu\text{m}^2 \text{s}^{-1}$), for linear colloidal chains as a function of the number of bonds N , where $N + 1$ is the number of droplets in the chain. Error bars are the standard error from measurements of many polymers and time points. (a) and (b) are derived from an analysis of 22 096 different polymers, while (c) is derived from an analysis of 7119 polymers. Insets show the scaling relations on a log-log plot.

angular displacement $\Delta\theta(t)$, we fit $-\ln \langle \cos \Delta\theta(t) \rangle$, which grows as $D_{\text{rot}} t$ with time, where D_{rot} is the rotational diffusion coefficient (see Ref. [26]). This expression accounts for the bounded nature of the angles. This generalized law for angular diffusion reduces to the law for translational diffusion, $\langle \Delta\theta^2 \rangle \simeq 2D_{\text{rot}} t$, for small $\Delta\theta$.

Figure 5(b) shows that the measured D_{rot} does not depend on the concentration C_{DNA} . For our $3 \mu\text{m}$ droplets, the average value of $D_{\text{rot}} = 0.008 \text{ rad}^2 \text{ s}^{-1}$ corresponds to a translational diffusion coefficient of $D_T = 0.07 \mu\text{m}^2 \text{ s}^{-1}$. This value is of the same order of magnitude as the measured diffusion coefficient of a single monomer, $D_m = 0.12 \pm 0.03 \mu\text{m}^2 \text{ s}^{-1}$, and similar to previously reported values [42]. We conclude that the reorganization of bonds in space is dominated by the diffusion of the droplet in the fluid, rather than the DNA patch sliding around on the droplet surface. The uniform distribution in Fig. 5(a) also implies that the Kuhn length b of our polymers is the distance between two bound droplets, i.e., the diameter.

Considering only linear colloidal chains from all C_{DNA} conditions, we characterize the structure of ≈ 22000 chains of lengths ranging from dimers to twentyimers. Figures 6(a), 6(b) show the sublinear growth of the root-mean-square end-to-end distance, $R_e = \sqrt{\langle \mathbf{R}^2 \rangle}$, and the radius of gyration R_g , where

$$R_g^2 = \frac{1}{(N+1)^2} \sum_{0 \leq i < j \leq N} \langle r_{ij}^2 \rangle \quad (1)$$

as a function of the number of bonds N and the number of droplets $N + 1$ in a colloidal chain, respectively. Each point is an ensemble average (in time and space) over thousands of polymers, ensuring ergodic sampling of the configurational space. The error bar increases with chain length because there are fewer long chains.

We find that both size parameters scale in good agreement with the Flory theory of a self-avoiding polymer [43], which happens to be exact in two dimensions [44], as $R_e = bN^\nu$ and $R_g = abN^\nu$, where α is a unitless constant,

b corresponds to the Kuhn length, and $\nu = 3/4$. A real polymer can be treated as an ideal polymer of N segments with length equal to the Kuhn length. Specifically, fits to the data yield $b = 1.0 \pm 0.03$ diameter, $\alpha = 0.3 \pm 0.02$, and exponents $\nu = 0.72 \pm 0.03$ and 0.79 ± 0.02 for R_e and R_g , respectively. A measurement of $b = 1$ droplet diameter confirms that the Kuhn length is one droplet. It is surprising that short chains already obey the scaling law that is supposed to apply in the asymptotic $N \rightarrow \infty$ limit only. One explanation is that the Ginzburg parameter is at its upper limit [45]. The Ginzburg parameter for a polymer chain in d dimensions is given by the ratio v/b^d , where v is the excluded volume of a monomer and b is the segment length [46]. In our case, the segment length is very nearly equal to the diameter of the excluded area. Accordingly, unlike regular polymers and particularly semiflexible ones (e.g., dsDNA), our colloidal chains exhibit no regime of polymer chain length with marginal self-avoidance. Therefore, the large N scaling is visible beginning with the shortest of chains and agrees with scaling laws in molecular polymers, including DNA [18] in the large N limit. Future work will investigate the scaling in three dimensions using density matched chains.

Next, we measure the dynamics of the colloidal chain through the diffusion of its center of mass. Our system consists of micron-sized droplets rearranging in a fluid, which implies hydrodynamic correlations between the monomers. The diffusion of a coil is described by the Zimm theory, which predicts that the diffusion coefficient scales as $D \propto (N+1)^{-\nu}$ [47]. Since the chain does not move as a ball, but rather as a pancake in two dimensions, the exponent is predicted to be $\nu = 3/4$, just like in the cases of R_e and R_g , as long as the surrounding fluid is in three dimensions. Our data in Fig. 6(c) are best fit with $\nu = 0.71 \pm 0.11$.

In conclusion, this work shows that the mobility of DNA on the droplet surface allows for the self-assembly of colloidal, fully flexible polymers. The DNA-binder concentration controls the droplet valence, such that we

obtain colloidomers with chain lengths whose distribution agrees with random attachment. Their bulk synthesis allows us to demonstrate that they are freely jointed, and that their size and diffusion coefficient scale with the chain length in agreement with a self-avoiding polymer.

In the future, colloidomers will serve to build both jammed [48] and complex ordered phases, such as close-packed spirals, predicted by numerical simulations [49]. Even further, these colloidomers open the platform for the self-assembly of complex three-dimensional materials or soft structures via a biomimetic folding approach [50]. The higher valence emulsions assemble into fibrous colloidal gels, mimicking the structure of cytoskeletal actin or microtubule networks. Just as their structure is continuously reconfigured by the cell, the reversible nature of the droplet-droplet bond paves the path towards responsive soft matter.

The authors gratefully acknowledge insights by David Pine and Sascha Hilgenfeldt, as well as useful conversations with Etienne Ducrot and Matan Yah Ben Zion. This work was supported by the Materials Research Science and Engineering Center (MRSEC) program of the National Science Foundation under Grants No. NSF DMR-1420073, No. NSF PHY17-48958, and No. NSF DMR-1710163. H.-C. was partially supported by Department of Energy Grant No. DE-SC0012296 and the Alfred P. Sloan Foundation. F.S. is grateful to the CSMR at NYU for hospitality.

-
- [1] L. Feng, L.-L. Pontani, R. Dreyfus, P. Chaikin, and J. Brujic, *Soft Matter* **9**, 9816 (2013).
- [2] Y. Zhang, A. McMullen, L.-L. Pontani, X. He, R. Sha, N. C. Seeman, J. Brujic, and P. M. Chaikin, *Nat. Commun.* **8**, 21 (2017).
- [3] D. Zerrouki, J. Baudry, D. Pine, P. Chaikin, and J. Bibette, *Nature (London)* **455**, 380 (2008).
- [4] S. Sacanna, W. T. M. Irvine, P. M. Chaikin, and D. J. Pine, *Nature (London)* **464**, 575 (2010).
- [5] B. Biswas, R. K. Manna, A. Laskar, P. B. S. Kumar, R. Adhikari, and G. Kumaraswamy, *ACS Nano* **11**, 10025 (2017).
- [6] R. Dreyfus, J. Baudry, M. L. Roper, M. Fermigier, H. A. Stone, and J. Bibette, *Nature (London)* **437**, 862 (2005).
- [7] I. Coluzza, P. D. van Oostrum, B. Capone, E. Reimhult, and C. Dellago, *Soft Matter* **9**, 938 (2013).
- [8] L.-N. Zou, X. Cheng, M. L. Rivers, H. M. Jaeger, and S. R. Nagel, *Science* **326**, 408 (2009).
- [9] S. Tricard, E. Feinstein, R. F. Shepherd, M. Reches, P. W. Snyder, D. C. Bandarage, M. Prentiss, and G. M. Whitesides, *Phys. Chem. Chem. Phys.* **14**, 9041 (2012).
- [10] Z. Rozynek, M. Han, F. Dutka, P. Garstecki, A. Józefczak, and E. Luijten, *Nat. Commun.* **8**, 15255 (2017).
- [11] M. Z. Miskin and H. M. Jaeger, *Nat. Mater.* **12**, 326 (2013).
- [12] H. R. Vutukuri, A. F. Demirörs, B. Peng, P. D. van Oostrum, A. Imhof, and A. van Blaaderen, *Angew. Chem.* **124**, 11411 (2012).
- [13] M. Z. Miskin and H. M. Jaeger, *Soft Matter* **10**, 3708 (2014).
- [14] R. S. Hoy, *Phys. Rev. Lett.* **118**, 068002 (2017).
- [15] P. Song, Y. Wang, Y. Wang, A. D. Hollingsworth, M. Weck, D. J. Pine, and M. D. Ward, *J. Am. Chem. Soc.* **137**, 3069 (2015).
- [16] D. E. Smith, T. T. Perkins, and S. Chu, *Macromolecules* **29**, 1372 (1996).
- [17] C. Bustamante, J. F. Marko, E. D. Siggia, and S. Smith, *Science* **265**, 1599 (1994).
- [18] B. Maier and J. O. Rädler, *Phys. Rev. Lett.* **82**, 1911 (1999).
- [19] A. A. Shah, B. Schultz, W. Zhang, S. C. Glotzer, and M. J. Solomon, *Nat. Mater.* **14**, 117 (2015).
- [20] I. Chakraborty, V. Meester, C. van der Wel, and D. J. Kraft, *Nanoscale* **9**, 7814 (2017).
- [21] C. van der Wel, G. L. van de Stolpe, R. W. Verweij, and D. J. Kraft, *J. Phys. Condens. Matter* **30**, 094005 (2018).
- [22] S. A. van der Meulen and M. E. Leunissen, *J. Am. Chem. Soc.* **135**, 15129 (2013).
- [23] D. Joshi, D. Bargeil, A. Caciagli, J. Burelbach, Z. Xing, A. S. Nunes, D. E. Pinto, N. A. Araújo, J. Brujic, and E. Eiser, *Sci. Adv.* **2**, e1600881 (2016).
- [24] L. Cademartiri and K. J. M. Bishop, *Nat. Mater.* **14**, 2 (2015).
- [25] N. A. Elbers, J. Jose, A. Imhof, and A. van Blaaderen, *Chem. Mater.* **27**, 1709 (2015).
- [26] See Supplemental Material at <http://link.aps.org/supplemental/10.1103/PhysRevLett.121.138002> for details on methods and the branching model.
- [27] L. Feng, B. Laderman, S. Sacanna, and P. Chaikin, *Nat. Mater.* **14**, 61 (2015).
- [28] N. Kern and D. Frenkel, *J. Chem. Phys.* **118**, 9882 (2003).
- [29] M. Y. Ben Zion and C. C. Maass, Conditional DNA Sequence Generator," (to be published).
- [30] Y. Wang, Y. Wang, X. Zheng, E. Ducrot, M.-G. Lee, G.-R. Yi, M. Weck, and D. J. Pine, *J. Am. Chem. Soc.* **137**, 10760 (2015).
- [31] N. J. Agard, J. A. Prescher, and C. R. Bertozzi, *J. Am. Chem. Soc.* **126**, 15046 (2004).
- [32] G. V. Dubacheva, C. Araya-Callis, A. Geert Volbeda, M. Fairhead, J. Codeé, M. Howarth, and R. P. Richter, *J. Am. Chem. Soc.* **139**, 4157 (2017).
- [33] M. Hadorn, E. Boenzli, K. T. Sørensen, H. Fellermann, P. Eggenberger, and M. M. Hanczyc, *Proc. Natl. Acad. Sci. U.S.A.* **109**, 20320 (2012).
- [34] L. Pontani, I. Jorjadze, V. Viasnoff, and J. Brujic, *Proc. Natl. Acad. Sci. U.S.A.* **109**, 9839 (2012).
- [35] S. Angioletti-Uberti, P. Varilly, B. M. Mognetti, and D. Frenkel, *Phys. Rev. Lett.* **113**, 128303 (2014).
- [36] P. A. Janmey, M. E. McCormick, S. Rammensee, J. L. Leight, P. C. Georges, and F. C. MacKintosh, *Nat. Mater.* **6**, 48 (2007).
- [37] J. Crocker and D. Grier, *J. Colloid Interface Sci.* **179**, 298 (1996).
- [38] G. Grimmett and D. Stirzaker, *Probability and Random Processes* (Oxford University Press, New York, 2001), p. 171.
- [39] B. Ruzicka, E. Zaccarelli, L. Zulian, R. Angelini, M. Sztucki, A. Moussaïd, T. Narayanan, and F. Sciortino, *Nat. Mater.* **10**, 56 (2011).
- [40] S. Corezzi, D. Fioretto, and F. Sciortino, *Soft Matter* **8**, 11207 (2012).

- [41] D. Y. Zhang and E. Winfree, *J. Am. Chem. Soc.* **131**, 17303 (2009).
- [42] R. W. Perry, M. C. Holmes-Cerfon, M. P. Brenner, and V. N. Manoharan, *Phys. Rev. Lett.* **114**, 228301 (2015).
- [43] P. J. Flory, *Principles of Polymer Chemistry* (Cornell University Press, Ithaca, NY, 1953).
- [44] P.-G. De Gennes, *Scaling Concepts in Polymer Physics* (Cornell University Press, Ithaca, NY, 1979).
- [45] K. Kremer, A. Baumgärtner, and K. Binder, *Z. Phys. B* **40**, 331 (1981).
- [46] A. Y. Grosberg and A. R. Khokhlov, *Statistical Physics of Macromolecules* (AIP Press, New York, 1994).
- [47] B. H. Zimm, *J. Chem. Phys.* **24**, 269 (1956).
- [48] E. Brown, A. Nasto, A. G. Athanassiadis, and H. M. Jaeger, *Phys. Rev. Lett.* **108**, 108302 (2012).
- [49] H. T. Nguyen, T. B. Smith, R. S. Hoy, and N. C. Karayiannis, *J. Chem. Phys.* **143**, 144901 (2015).
- [50] Z. Zeravcic, V. N. Manoharan, and M. P. Brenner, *Proc. Natl. Acad. Sci. U.S.A.* **111**, 15918 (2014).